



0040-4020(95)00489-0

## Structure of the 1:1 Cycloadduct Formed via Thermal Reaction of Cyclopentadiene with Hexacyclo[10.2.1.0<sup>2,11</sup>.0<sup>4,9</sup>.0<sup>4,14</sup>.0<sup>9,13</sup>]pentadeca-5,7-diene-3,10-dione<sup>†</sup>

Alan P. Marchand\*, Rajesh Shukla, Andrew Burritt, and Simon G. Bott\*

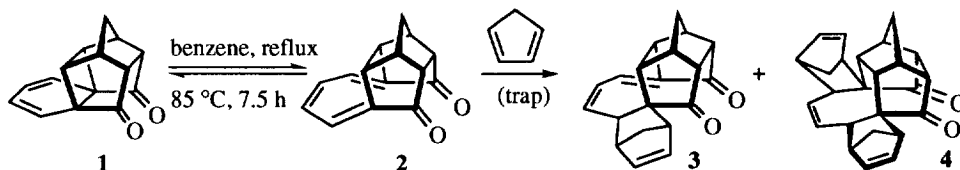
Department of Chemistry, University of North Texas, Denton, Texas 76203-0068

*Key words:* Diels-Alder cycloaddition;  $\pi$ -facial diastereoselectivity; MO calculations

**Abstract.** The structure of the 1:1 cycloadduct which is formed via thermal reaction of cyclopentadiene (CPD) with hexacyclo[10.2.1.0<sup>2,11</sup>.0<sup>4,9</sup>.0<sup>4,14</sup>.0<sup>9,13</sup>]pentadeca-5,7-diene-3,10-dione (**1**) has been shown unequivocally to possess structure **3b** via application of X-ray crystallographic methods. The results of semiempirical MO calculations (AM1 Hamiltonian), taken together with MMX calculational results and conclusions that arise via FMO-based arguments, suggest that electronic and steric effects each may play an important role in directing the course of the cycloaddition reactions studied herein.

**Introduction.** Recently, hexacyclo[10.2.1.0<sup>2,11</sup>.0<sup>4,9</sup>.0<sup>4,14</sup>.0<sup>9,13</sup>]pentadeca-5,7-diene-3,10-dione (**1**) has attracted considerable attention as an example of a  $\pi$ -facially differentiated Diels-Alder diene which readily enters into thermal [4 + 2] cycloadditions to a variety of dienophiles.<sup>1</sup> The corresponding Diels-Alder cycloaddition of **1** with cyclopentadiene (CPD) has been studied previously.<sup>2,3</sup> Interestingly, **1** undergoes thermal six-electron electrocyclic ring opening prior to its reaction with CPD. The resulting triene, **2** (Scheme 1), subsequently functions as the *dienophile* component when it undergoes thermal [4 + 2] cycloaddition to CPD; this reaction produces both the corresponding [4 + 2] monocycloadduct (**3**)<sup>2,3</sup> and bis-cycloadduct (**4**)<sup>2</sup>.

Scheme 1

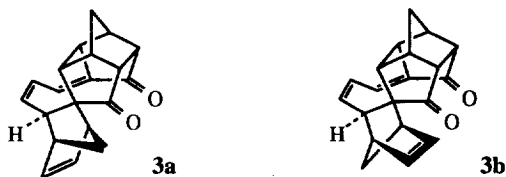


The gross structure of **3** was arrived at via analysis of its one- and two-dimensional NMR spectra. However, this approach failed to distinguish between two structural alternatives, i. e., **3a** and **3b** (Scheme 2), which were not explicitly considered.<sup>3</sup> In order to resolve this ambiguity, we repeated the Diels-Alder reaction of CPD with **1**, isolated the 1:1 [4 + 2] cycloadduct, and obtained unequivocal verification of its structure, **3b**,

<sup>†</sup>Dedicated to Professor Yoshito Takeuchi on the occasion of his 60th birthday.

by application of X-ray crystallographic methods. In addition, we have used semiempirical MO computational methods to further investigate some aspects of the mechanism of cycloaddition of CPD to **1**.

Scheme 2



**Results of Theoretical Calculations.** Two issues were considered when addressing theoretical aspects of the thermal reaction of CPD with **1**: (i) the energetics of thermal electrocyclic ring opening of **1** to **2** and (ii) the relative energetics of Diels-Alder cycloaddition of CPD to **1** vs. the corresponding reaction with **2**. Semiempirical molecular orbital (MO) calculations (AM1 Hamiltonian)<sup>4</sup> were performed by using readily available computational software (MOPAC<sup>5</sup> and SPARTAN<sup>6</sup> (see the Experimental Section). Diels-Alder transition structures were located by using RHF theory and by assuming that a concerted mechanism is operative.<sup>7</sup> A similar approach was used to examine electrocyclic ring opening of **1** to **2** (*vide infra*).

Two possible reaction pathways were considered explicitly for thermal electrocyclic ring opening of **1** to **2**, i. e., one which leads to formation of "Z,Z,Z-triene" (**2a**) and another which affords the corresponding "E,Z,E-triene" (**2b**). The results of semiempirical MO calculations (AM1) for this process are summarized in Figure 1. Here, the energies shown are relative to the heat of formation of **1**. The relative AM1 energies of the ring-opened product trienes indicate that **2a** is favored thermodynamically relative to **2b** by *ca.* 24 kcal·mol<sup>-1</sup>. The relatively large difference in energy requirements between the two pathways for thermal electrocyclic ring-opening of **1** is reflected in the relative energies of their respective transition structures. Thus, the transition structure for electrocyclic ring opening of **1** to **2a** (i. e., **5a**) is predicted to be *ca.* 22 kcal·mol<sup>-1</sup> lower in energy than the corresponding transition structure for electrocyclic ring opening of **1** to **2b** (i. e., **5b**; see Figure 1). It follows that any subsequent reaction which involves the ring-opened cage triene formed from **1** is more likely to proceed via **2a** than **2b**.

Next, two possible modes of Diels-Alder cycloaddition of CPD to triene **2a** were considered. In one case, CPD is allowed to approach the "outside" face of the reacting C=C double bond in **2a** in such a way that the vinyl C-H bond in the dienophile becomes situated on the *endo* face of the newly formed norbornene ring in the product, **3a**. Alternatively, the approach of CPD to the dienophile might proceed to afford cycloadduct **3b** in which this same C-H bond now occupies the *exo* face of the newly-formed norbornene ring. The results of AM1 calculations for these two processes are shown in Figure 2. When both kinetic and thermodynamic considerations are taken into account, there appears to be a clear preference for formation of **3b** *vis-à-vis* **3a**, in agreement with experimental observations.

Finally we considered four possible modes of Diels-Alder cycloaddition of CPD to **1**. The results of AM1 calculations are shown in Figure 3. It will be noted that the energy required to traverse any of the four transition states (**7a-7d**) is significantly greater than for *either* of the two pathways depicted in Figure 2 for the corresponding cycloaddition of CPD to ring-opened triene **2a**. In particular, the activation barrier for

cycloaddition of CPD to **2a** (Figure 2) to afford the observed product, **3b**, is *ca.* 6.5 kcal·mol<sup>-1</sup> lower in energy than the lowest energy pathway for addition to diene **1** (TS **7a**, Figure 3).

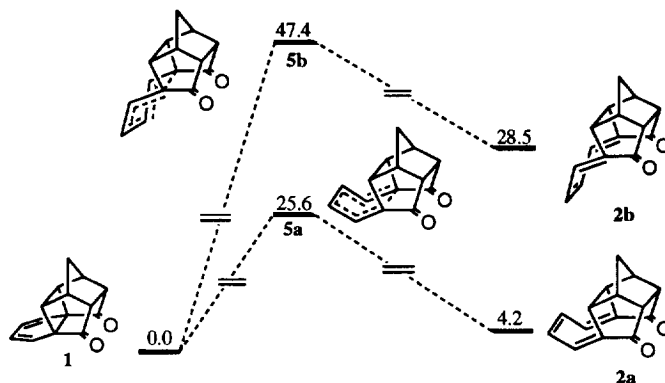


**Figure 1.** Results of AM1 calculations for two possible modes of thermal six-electron electrocyclic ring-opening of **1**. Energies are expressed in kcal·mol<sup>-1</sup> relative to **1**.

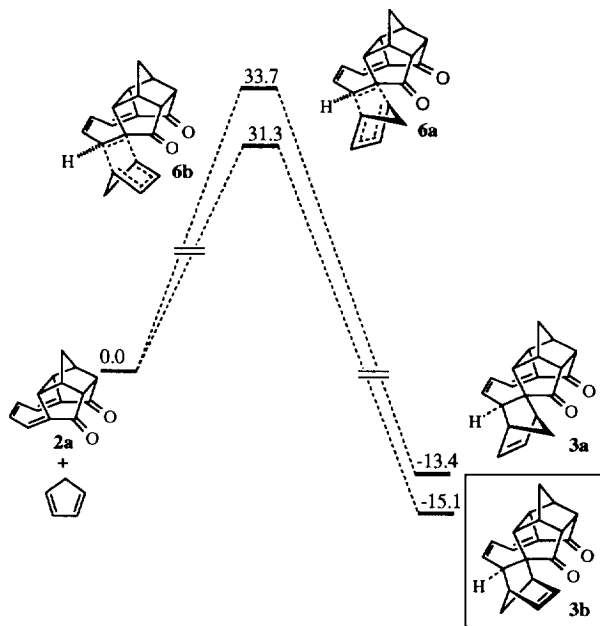


**Figure 2.** Results of AM1 calculations for two possible modes of Diels-Alder cycloaddition of cyclopentadiene to **2a**. Energies are expressed in kcal·mol<sup>-1</sup> relative to **2a** and CPD.

It should be noted that a significant energy barrier must be traversed in order for cage diene **1** to undergo valence isomerization to triene **2a** (i. e., *ca.* 25 kcal·mol<sup>-1</sup>). Nevertheless, if **1** and **2a** are in equilibrium with one another, then the results of our AM1 calculations suggest that CPD is expected to undergo [4 + 2] cycloaddition preferentially with **2a** *vis-à-vis* the corresponding reaction with **1**.

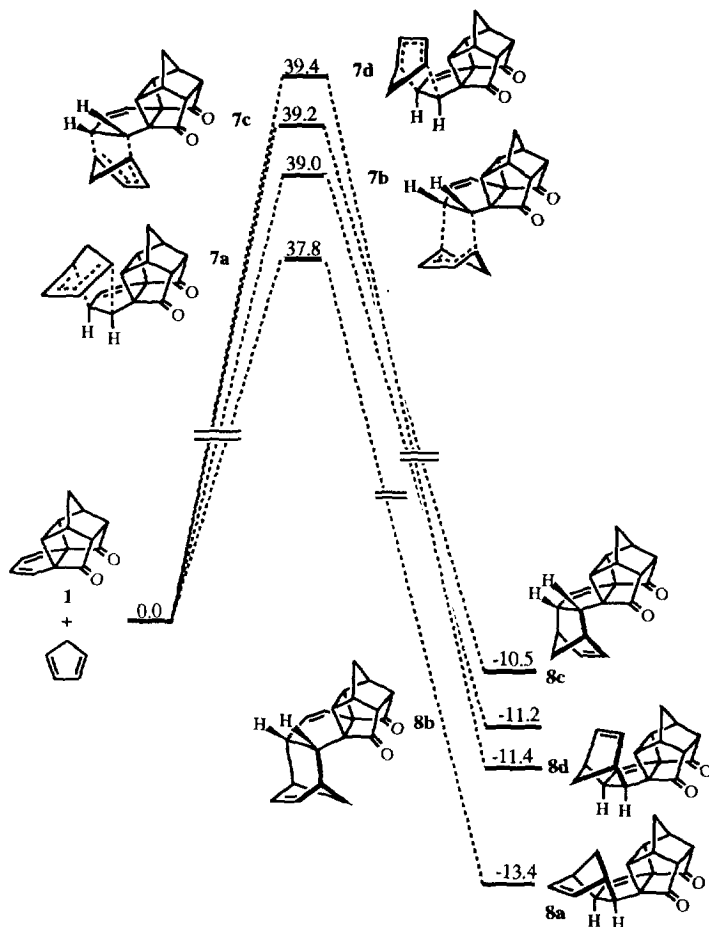


**Figure 3.** Results of AM1 calculations for the four possible modes of Diels-Alder cycloaddition of CPD (diene) to **1** (dienophile). Energies are expressed in  $\text{kcal}\cdot\text{mol}^{-1}$  relative to **1** and CPD.

The results of AM1 calculations suggest that the thermodynamically favored product of [4 + 2] cycloaddition of CPD to **1** should be **8a**. Nevertheless, **8a** is *not* the experimentally observed product of this reaction, despite the fact that the AM1 calculations predict **8a** to be *ca.*  $2.5 \text{ kcal}\cdot\text{mol}^{-1}$  more stable than the observed reaction product, **3b** (*cf.* Figures 2 and 3). Relevant energetics are summarized in Figure 4. This result suggests that the course of the thermal reaction of CPD with **1** is *not* determined by (thermodynamic) product stability but instead reflects the relative dienophilic (kinetic) reactivities of **1** vs. **2a** toward CPD.

**Frontier Molecular Orbital Analysis.** Consideration of the differences between the HOMO and LUMO orbitals for CPD-**1** and CPD-**2a** diene-dienophile interactions should afford a reasonable representation of the potential for HOMO-LUMO interactions and, hence, the degree of stabilization which can be attained via orbital mixing. The following HOMO and LUMO values were calculated at the HF/3-21G(\*) level of theory [HOMO (eV), LUMO (eV)] for **1**, **2a**, and CPD, respectively: -8.39, 3.07; -9.60, 2.39; -8.48, 3.89.

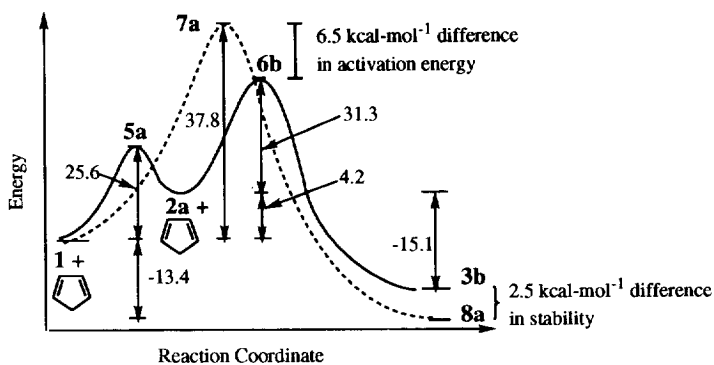


**Figure 4.** Reaction coordinate diagram for the lowest energy modes of cycloaddition of cyclopentadiene to cage diene **1** and to ring-opened triene **2a**.

At the AM1 level of theory, **1** and **2a** were calculated to possess slightly negative LUMO energies (-0.03 and -0.38 eV, respectively). When the geometries of **1** and **2a** instead were optimized at the HF/3-21G(\*) level of theory, the LUMO energies were found to be distinctly positive (*vide supra*). The differences between the LUMO and HOMO orbital energies of CPD/**1** and CPD/**2a** diene/dienophile interactions ( $\Delta E = E_{\text{LUMO}} - E_{\text{HOMO}}$ ), calculated at the HF/3-21G(\*) level of theory, are as follows:  $\Delta E$  (CPD<sub>LUMO</sub> - **1**<sub>HOMO</sub>) = 12.28 eV;  $\Delta E$  (CPD<sub>LUMO</sub> - **2a**<sub>HOMO</sub>) = 13.49 eV;  $\Delta E$  (**1**<sub>LUMO</sub> - CPD<sub>HOMO</sub>) = 11.55 eV;  $\Delta E$  (**2a**<sub>LUMO</sub> - CPD<sub>HOMO</sub>) = 10.87 eV.

According to Frontier Molecular Orbital theory (FMO), the smaller the differences between HOMO-LUMO energies, the lower will be the energy of the newly-formed filled orbital in the species which results from these orbital interactions. For Diels-Alder cycloadditions of CPD to **1** and to **2a**, the smallest difference in orbital energies (10.87 eV) occurs via mixing between the HOMO of CPD and the LUMO of **2a**. Hence, Diels-Alder cycloaddition of CPD to **2a** is expected to result in greater stabilization of the forming filled molecular orbital in the transition structure which leads to cycloadduct **3b** than would be achieved if CPD instead were to cycloadd directly to **1**. Again, the computational results are in agreement with experiment, as **3b** is indeed the only Diels-Alder cycloadduct to result from thermal reaction of CPD with **1**.

The steric energies of transition structures **6a**, **6b**, and **7a-7d** were calculated (MMX)<sup>8</sup> for both the fixed AM1 geometry and the corresponding MMX optimized geometry. The results of these calculations (Table 1) indicate that in both cases, the steric energy incurred as a result of [4 + 2] cycloaddition of CPD to triene **2a** is less than that for the corresponding cycloaddition of CPD to diene **1**.

**Table 1.** Results of MMX calculations

Structure	MMX energy of AM1 optimized geometry (kcal-mol <sup>-1</sup> )	MMX optimized TS geometry (kcal-mol <sup>-1</sup> )	Structure	MMX energy of AM1 optimized geometry (kcal-mol <sup>-1</sup> )	MMX optimized TS geometry (kcal-mol <sup>-1</sup> )
<b>6a</b>	109.5	56.4	<b>7b</b>	148.1	78.3
<b>6b</b>	113.3	56.0	<b>7c</b>	148.9	76.3
<b>7a</b>	150.3	77.6	<b>7d</b>	150.3	78.1

### Experimental Section

Melting points are uncorrected. Elemental microanalyses were performed at M-H-W Laboratories, Phoenix, AZ. Compound **3b** was synthesized by using a procedure which has been described previously.<sup>3</sup>

**Computational Methods.** Calculations were performed by using MOPAC,<sup>5</sup> version 6.0 or SPARTAN,<sup>6</sup> version 3.1 with the AM1 Hamiltonian.<sup>4</sup> MOPAC calculations were carried out with the keyword PRECISE in all cases, and transition structures were located by using the keyword TS. Calculations in SPARTAN were performed by using the default convergence and optimization criteria for the selected type of stationary point to be located. MMX calculations (Table 1) were performed by using PCMODEL.<sup>8</sup>

**X-ray Structure of 3b.** All data were collected on a colorless crystal of C<sub>20</sub>H<sub>18</sub>O<sub>2</sub> of dimensions 0.42 x 0.51 x 0.54 mm. All measurements were made on an Enraf-Nonius CAD-4 diffractometer with graphite monochromated Mo K $\alpha$  radiation ( $\lambda = 0.71073$  Å),  $\mu = 0.80$  cm<sup>-1</sup>, by using the  $\omega$  scan technique,  $2\theta_{\max} = 44^\circ$ . Standard procedures in our laboratory have been described previously.<sup>9</sup> A total of 3971 reflections were collected, all of which were unique. Data were corrected for Lorentz and polarization effects, but not for absorption. The structures were solved by direct methods (SHELX86).<sup>10</sup> The final cycle of full-matrix, least squares refinement was based on 2066 observed reflections [ $I \geq 3\sigma(I)$ ] and 287 variables, for which  $R = 0.0543$  and  $R_w = 0.0525$ . Due to a lack of data, only the oxygen and non-cage carbon atoms were refined with anisotropic thermal parameters, the rest of the non-hydrogen atoms being isotropic. Hydrogen atoms were located on difference maps and then included in the model in idealized positions [U(H) = 1.3 Beq(C)]. The maximum and minimum peaks on the final difference Fourier map corresponded to 0.27 and -0.26 e-Å<sup>-3</sup>, respectively. All computations other than those specified were performed by using MolEN.<sup>11</sup> Scattering factors were taken from the usual sources.<sup>12</sup> Cell constants: space group Pbcn,  $a = 29.088$  (2),  $b = 8.5975$  (6),  $c = 22.808$  Å;  $V = 5703.9$  (7) Å<sup>3</sup>. For  $Z = 16$  and a formula weight of 290.4,  $D_{\text{calc}} = 1.352$  g-cm<sup>-3</sup>. The asymmetric unit consists of two independent molecules which show no significant differences.

**Acknowledgment.** This work was supported by the Office of Naval Research (Grant N00014-94-1-1039 to A. P. M.), the U. S. Air Force (Contract F29601-92-K-0018 to A. P. M.), the Robert A. Welch Foundation (Grants B-963 to A. P. M., B-1202 to S. G. B.), and the UNT Faculty Research Committee (S. G. B.).

### References and Footnotes

1. See: Coxon, J. M.; Fong, S. T.; Lundie, K.; McDonald, D. Q.; Steel, P. J.; Marchand, A. P.; Zaragoza, F.; Zope, U. R.; Rajagopal, D.; Bott, S. G.; Watson, W. H.; Kashyap, R. *Tetrahedron* **1994**, *50*, 13037 and references cited therein.
2. Coxon, J. M.; O'Connell, M. J.; Steel, P. J. *J. Org. Chem.* **1987**, *52*, 4726.
3. Mehta, G.; Singh, V.; Rao, K. S. *Tetrahedron Lett.* **1980**, *21*, 1369.
4. Dewar, M. J. S.; Zoebisch, E. G.; Healy, E. F.; Stewart, J. J. P. *J. Am. Chem. Soc.* **1985**, *107*, 3902.
5. MOPAC, version 6.0; Quantum Chemistry Program Exchange (QCPE), Program Number 455, **1990**.
6. SPARTAN, version 3.1; Wavefunction, Inc., 18401 Von Karman, Suite 370, Irvine, CA 92715.
7. (a) Storer, J. W.; Raimondi, L.; Houk, K. N. *J. Am. Chem. Soc.* **1994**, *116*, 9675. (b) Li, Y.; Houk, K. N. *J. Am. Chem. Soc.* **1993**, *115*, 7478. (c) Houk, K. N.; Li, Y.; Evanseck, J. D. *Angew. Chem., Int. Ed. Engl.* **1992**, *31*, 682.
8. PCMODEL, version 4.0; Serena Software, P. O. Box 3076, Bloomington, IN 47402-3076. Diels-Alder transition structure bond orders were assumed to be 0.3 for the forming carbon-carbon  $\sigma$ -bonds.
9. Mason, M. R.; Smith, J. M.; Bott, S. G.; Barron, A. R. *J. Am. Chem. Soc.* **1993**, *115*, 4971.
10. Sheldrick, G. M. In: *Crystallographic Computing*, Sheldrick, G. M.; Krüger, C.; Goddard, R., Eds.; Oxford University Press: Oxford, U. K., 1985; pp 184-189.
11. MolEN, *An Interactive Structure solution Program*; Enraf-Nonius: Delft, The Netherlands; 1990.
12. Cromer, D. T.; Waber, J. T. *International Tables for X-Ray Crystallography*; Kynoch Press: Birmingham; 1974; Vol. IV, Table 2.